Supplementary Material

New copper(II) and oxidovanadium(IV) complexes with a vitamin B_6 Schiff base: mechanism of action and synergy studies on 2D and 3D human osteosarcoma cell models.

Lucia M. Balsa [a], Valeria Ferretti [a], Marco Sottile [a], Patrique Nunes[b], João Costa Pessoa[b], Isabel Correia [b,*], Ignacio E. León[a,c*]

[a] CEQUINOR (UNLP, CCT-CONICET La Plata, asociado a CIC), Departamento de Química, Facultad de Ciencias Exactas, Universidad Nacional de La Plata. Blvd. 120 N° 1465, La Plata (1900), Argentina .

[b] Centro de Química Estrutural, Institute of Molecular Sciences, and Departamento de Engenharia Química, Instituto Superior Técnico, Av. Rovisco Pais 1, 1049-001 Lisboa, Portugal.

[c] Cátedra de Fisiopatología, Departamento de Ciencias Biológicas, Facultad de Ciencias Exactas, Universidad Nacional de La Plata. 47 y 115, La Plata 1900, Argentina

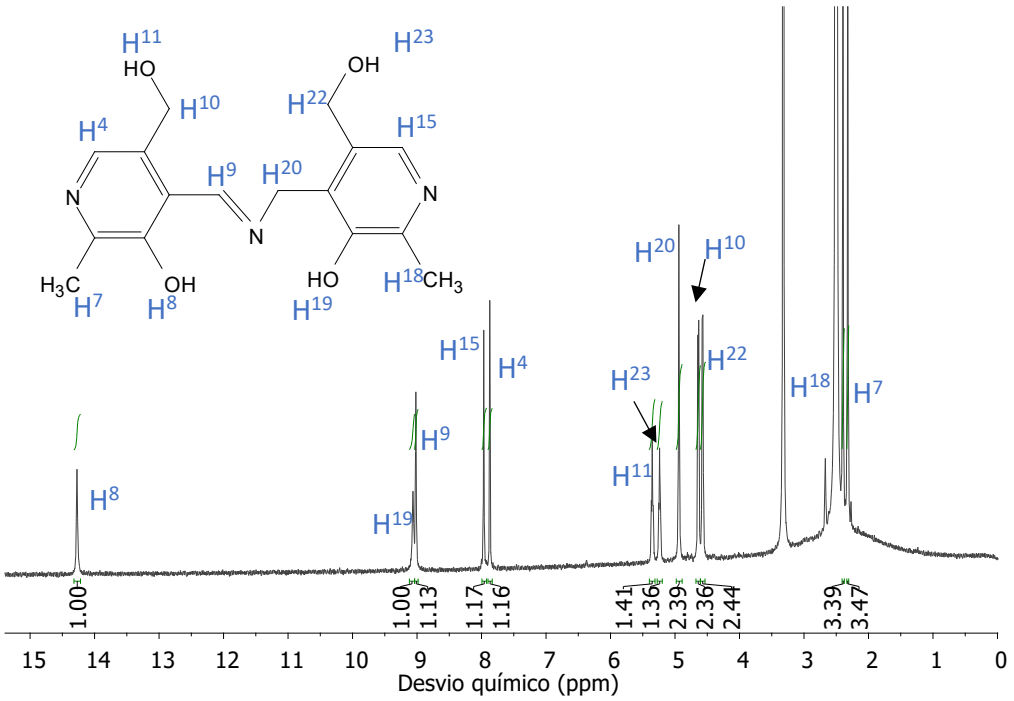

Figure S1. ^{1}H-NMR spectrum of H_2L in DMSO-d_6 with the atom labelling scheme and respective peak assignments.

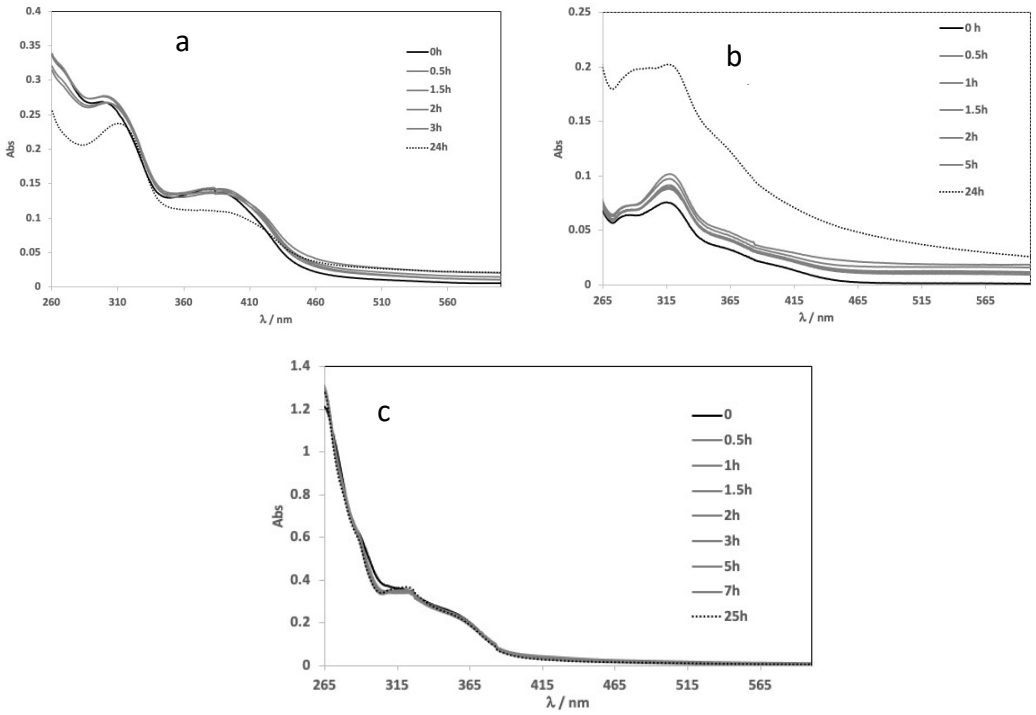

Figure S2. Electronic absorption spectra acquired within 24 h in PBS at room temperature measured for a) Complex **1**, [**1**] = 25 μM and 2.5% DMSO, b) complex **4**, [**4**] = 40 μM and 2.5% DMSO and c) complex **5**, [**5**] = 47 μM and 5% DMSO.

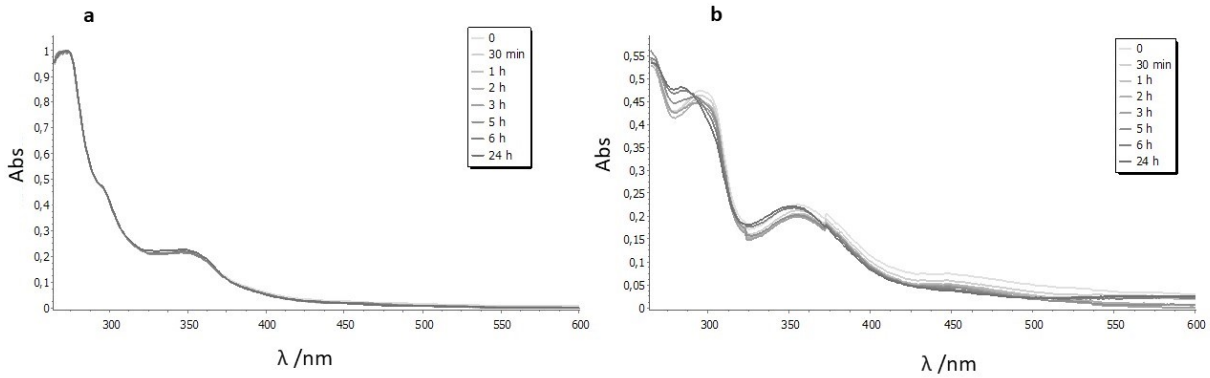

Figure S3. Electronic absorption spectra acquired within 24 h in DMSO at room temperature measured for a) complex **2**, [**2**] = 65 µM, b) complex **3**, [**3**] = 25 µM

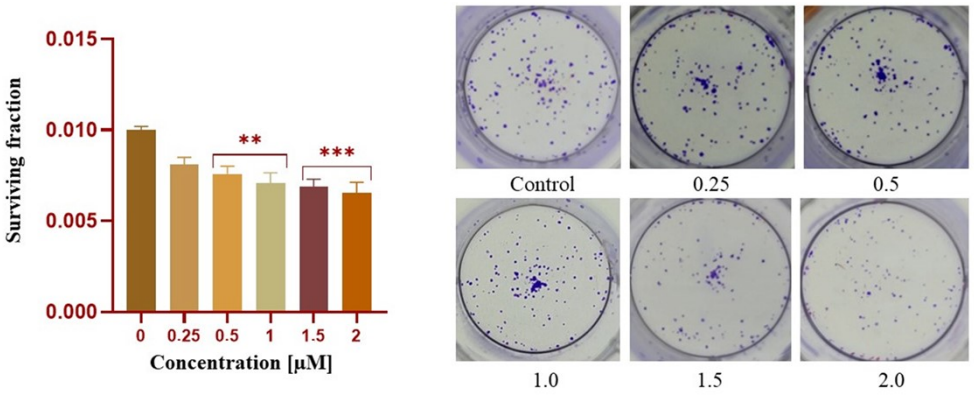

Figure S4. Clonogenic assay. Effect of complex **2** on MG-63 cell proliferation. Cells were incubated in Dulbecco's modified Eagle's medium (DMEM) alone (control), or with different concentrations (0.25 to 2.0 µM) of complex **2**. The results are expressed as surviving fraction as the percentage of the basal level and represent the mean ± the standard error of the mean (SEM) (n =18). ** = p-value < 0.001 *** = p-value < 0.0005 differences between control and treatment.

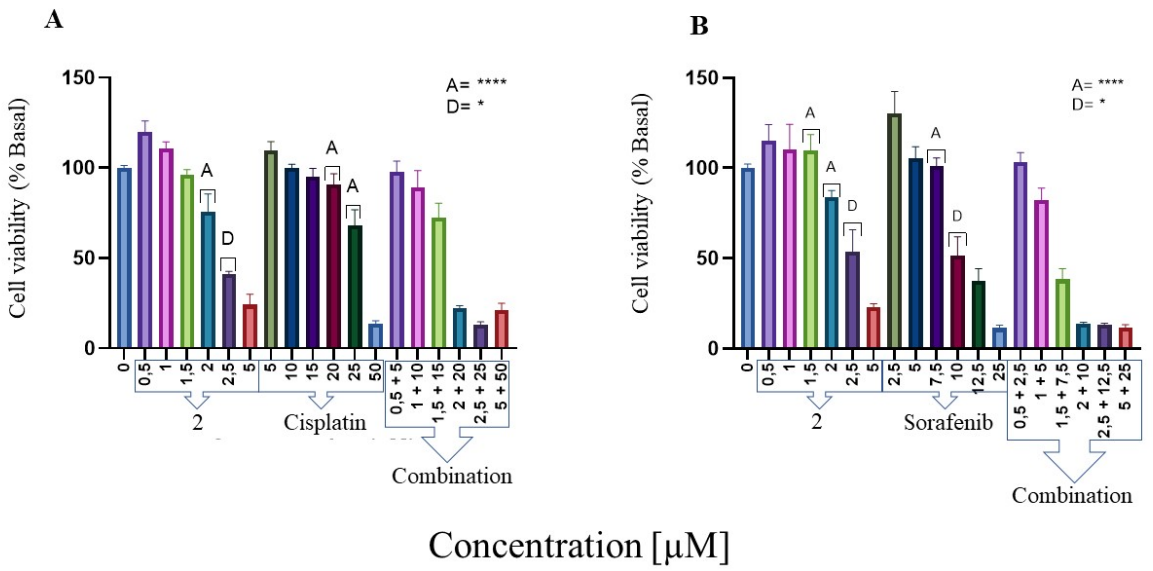

Figure S5. Synergy studies on MG-63. A) Complex **2** and cisplatin. B) Complex **2** and sorafenib, expressed in terms of cell viability.

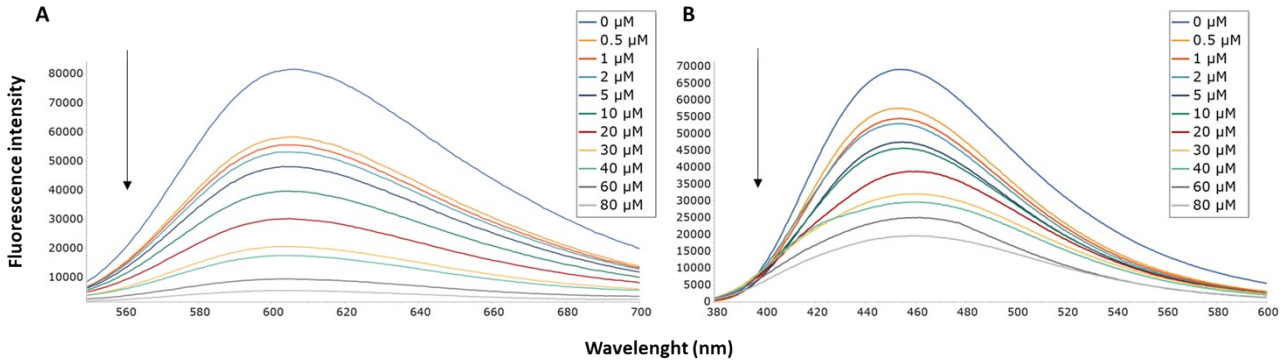

Figure S6. Fluorescence emission spectra (in arbitrary units) of EB (A) and DAPI (B) bound to CT-DNA in the untreated condition and in the presence of complex **2** (0.5–80 µM). The excitation wavelengths were 510 nm and 358 nm for EB and DAPI, respectively. The arrow indicates the decrease in fluorescence intensity of EB (A) and DAPI (B) bound CT-DNA with increasing concentration of complex **2**. The concentrations of EB, DAPI, and *calf thymus* DNA were 1 µM, 1 µM, and 10 µM, respectively.

A

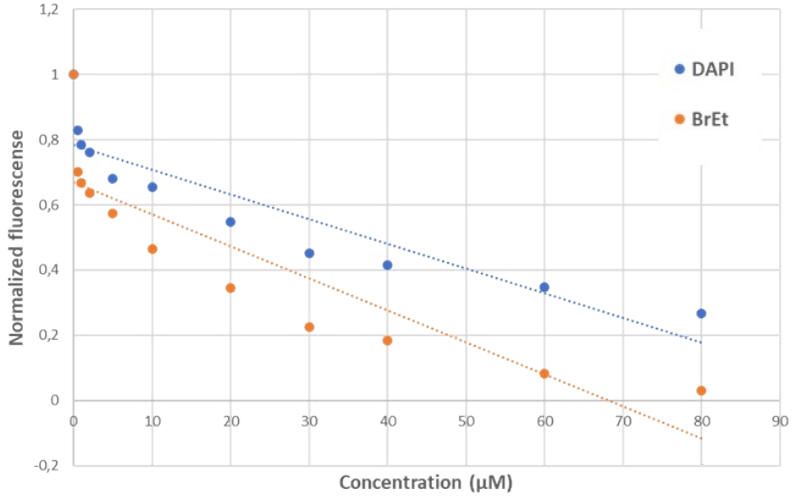

B

$C_{50}(I)$	$1.72x10^{-5}$
$C_{50}(G)$	$3.73x10^{-5}$
RI_{50}	$4.02x10^{5}$
RG_{50}	$1.60x10^{5}$
RI/RG	2,51
I%	71.5%

Figure S7. A) Plot of normalized fluorescence versus increasing concentration of complex **2**. B) Intercalative and grove DNA binding mode percentages of **2**.

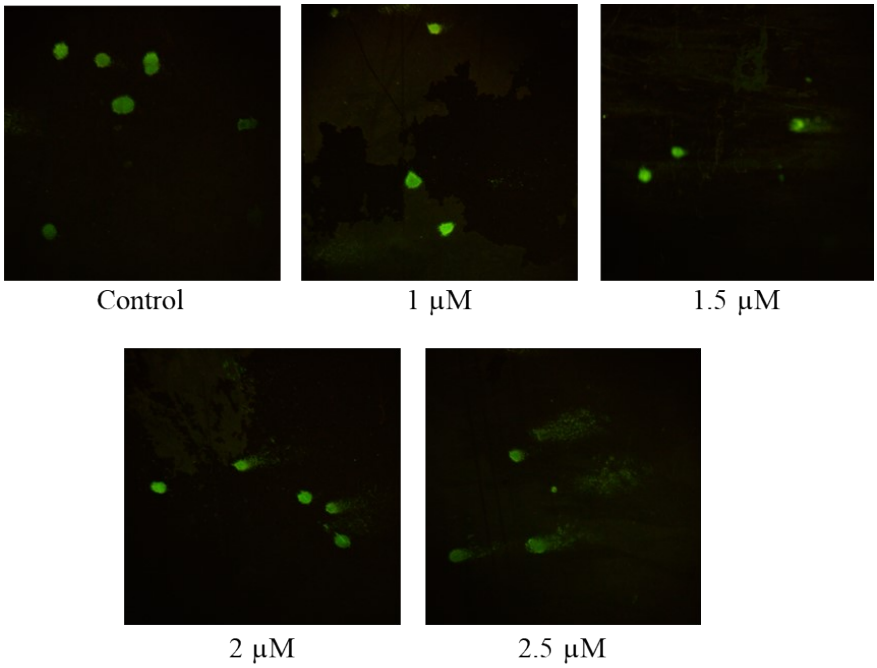

Figure S8. Genotoxicity of complex **2** on MG-63 cancer cells evaluated by the Comet assay at different concentrations.

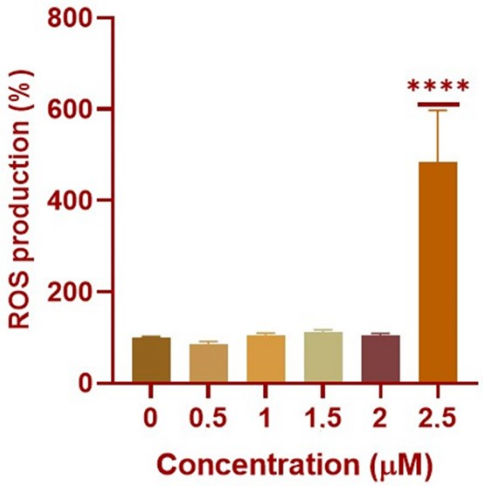

Figure S9. Induction of ROS generation by complex **2** on the MG-63 cells at 24 h. ROS production in the cells was evaluated through the oxidation of DHR123 to rhodamine 123 (by spectrofluorometry), and was normalized to micromole of rhodamine 123 per liter per milligram of protein (percentage of the basal value). The results represent the mean ± SEM (n = 12). The asterisk stands for the difference with respect to the control ($p < 0.01$).

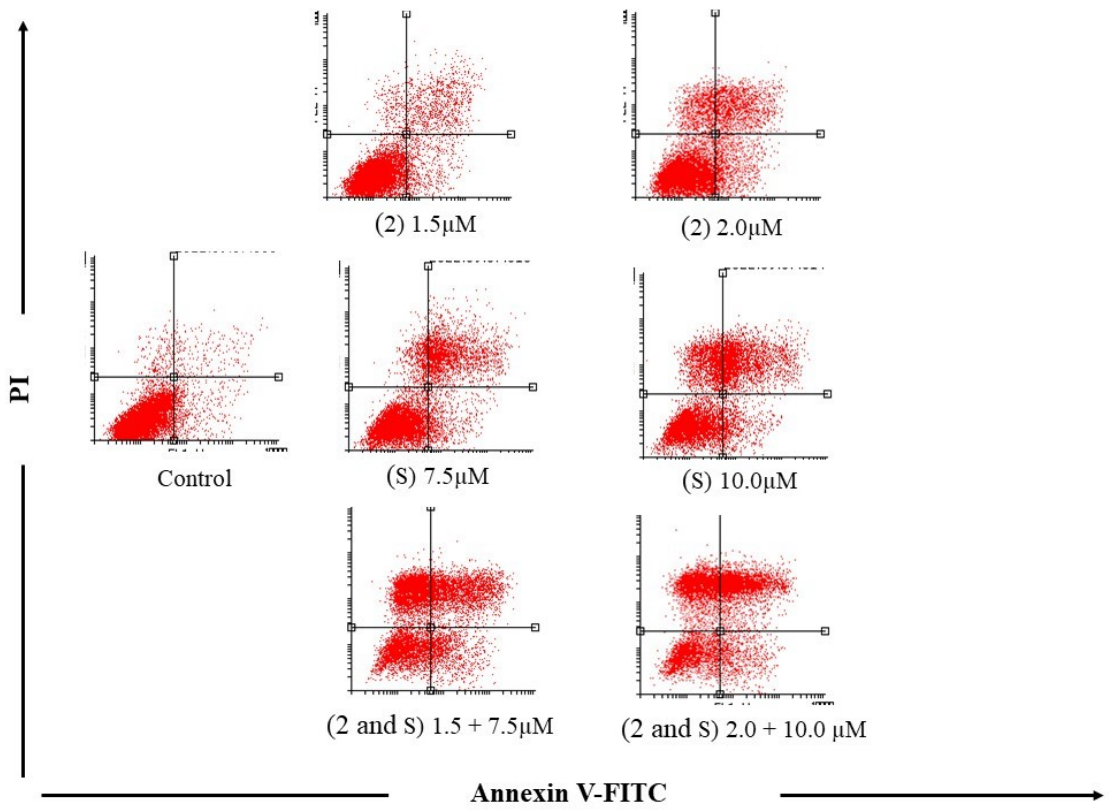

Figure S10. Apoptosis dot plot of MG-63 cells treated with complex **2** (1.0 and 2.0 µM), sorafenib (7.5 and 10.0 µM) and combination of **2** and sorafenib (1.0 + 7.5 and 2.0 + 10.0 µM), obtained by flow cytometry.

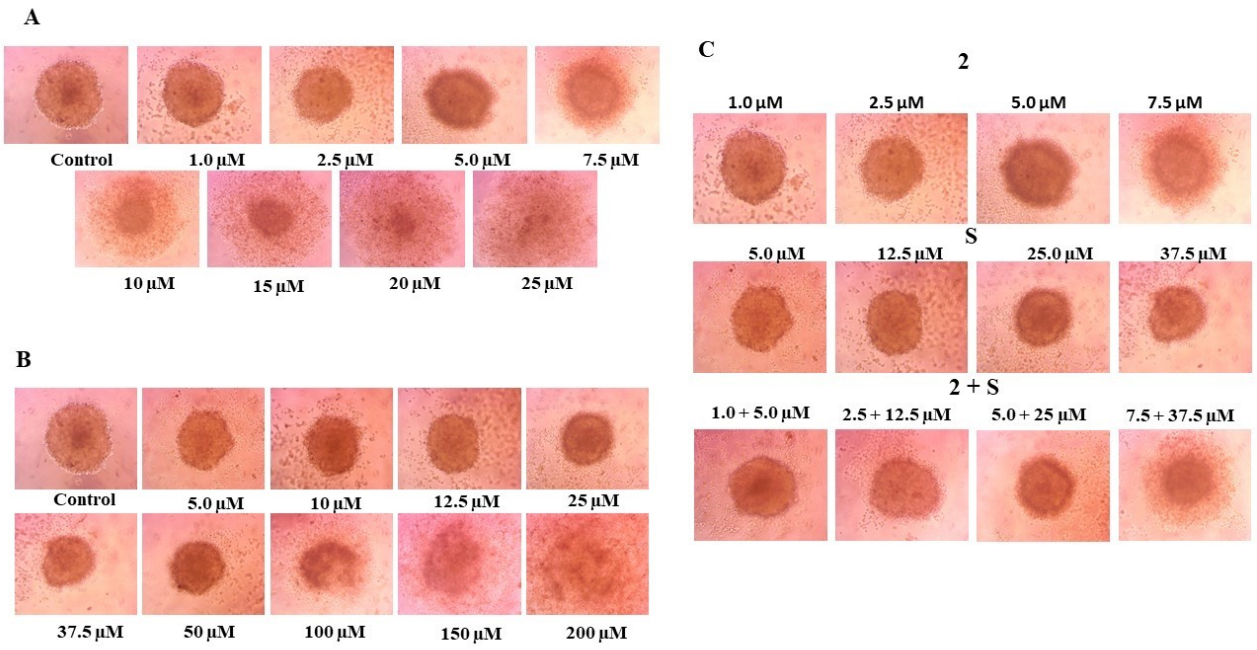

Figure S11. MG-63 spheroids cytotoxicity assay. Spheroids were treated with A) complex **2** (1.0 - 25 μM) B) sorafenib (5.0 - 200 μM) and C) combination of **2** and sorafenib (1.0-7.5/ 5.0-37.5 μM)